J|A|C|S
ARTICLES
Published on Web 12/14/2005

Encapsulation of Fluorescent Molecules by Functionalized Polymeric Nanocontainers: Investigation by Confocal Fluorescence Imaging and Fluorescence Correlation Spectroscopy

Per Rigler and Wolfgang Meier*

Contribution from the Physikalische Chemie, Universität Basel, Klingelbergstrasse 80, 4056 Basel, Switzerland

Received September 30, 2005; E-mail: wolfgang.meier@unibas.ch

Abstract: Nanocontainers (NCs) were prepared from amphiphilic triblock copolymers, having an average molecular weight of around 8000 g/mol, by using previously published preparation methods consisting of dispersing the polymer in an aqueous buffer solution containing molecules for encapsulation. A small molecular weight fluorophore, sulforhodamine B, as well as the fluorescent protein avidin labeled with Alexa 488 were encapsulated, and the resulting nanocontainers were characterized using fluorescence correlation spectroscopy (FCS) and fluorescence cross-correlation spectroscopy (FCCS). Nanocontainer size determination by FCS is very robust and compares well with results obtained from photon correlation spectroscopy: the measured diameters of the polymeric nanocontainers vary between 140 and 172 nm. Encapsulation of fluorescent molecules was determined by evaluating the molecular brightness of nanocontainers with an encapsulated fluorescently labeled protein (avidin−Alexa 488). Results indicate that the number of encapsulated avidin−Alexa 488 molecules corresponds well with the initial concentration of the fluorescently labeled protein and the encapsulated volume. A nanocontainer binding assay was developed using biotinylated fluorescently labeled nanocontainers. Binding of biotinylated nanocontainers to fluorescently labeled streptavidin was followed by fluorescence cross-correlation spectroscopy. The intrinsic dissociation constant, K_d, of labeled streptavidin to the ligand-modified nanocontainers is $1.7 \pm 0.4 \times 10^{-8}$ M, and about 1921 ± 357 molecules of labeled streptavidin are bound to each nanocontainer.

Introduction

Carrier-based drug delivery using lipid vesicle systems is an attractive approach to provide sustained release of a drug and to protect the drug moiety from immediate dilution. This might lead to less toxicity and greater therapeutic efficacy. Already in the mid-1960s Bangham and co-workers discovered that hydration of phospholipid films leads to the formation of vesicles with an inner aqueous compartment surrounded by a lipid bilayer.[1,2] It did not take long until these vesicles, also known as liposomes, were exploited as vehicles for drug delivery.[3−6] Throughout the years a great deal of interesting research has been conducted, but so far only a few liposome-based drugs have made it to the clinics. The reasons behind the unsatisfactory results obtained with lipid vesicles are the relatively high drug leakage rates of the encapsulated drug and the short circulation half-life in the blood stream.[7] Furthermore, chemical modification of lipid vesicles, a prerequisite for targeted drug delivery, is not straightforward.

Another important prerequisite for using vesicles for drug delivery is that the size and its corresponding distribution can be precisely tuned.[8−10] It is equally important to ensure an efficient and reproducible encapsulation of the active compound which up to now has been very difficult to analyze. To prevent early clearance from the blood stream via either opsonization or the mononuclear phagocyte system, and to enable ligand modification for targeting, the carrier should be strongly protein repellent and easy to modify chemically, respectively.

An interesting alternative to lipid vesicles in drug delivery is polymeric vesicles of block copolymers offering very versatile building blocks for a great variety of subsequent chemical modifications. Earlier work conducted with block copolymers shows that they behave very much like the lipidic counterpart:

(1) Bangham, A. D.; Horne, R. W. *J. Mol. Biol.* **1964**, *12*, 660−668.
(2) Bangham, A. D.; Standish, M. M.; Watkins, J. C. *J. Mol. Biol.* **1965**, *13*, 238−252.
(3) Papahadj, D.; Mayhew, E.; Poste, G.; Smith, S.; Vail, W. J. *Nature* **1974**, *252*, 163−166.
(4) Alving, C. R.; Steck, E. A.; Chapman, W. L.; Waits, V. B.; Hendricks, L. D.; Swartz, G. M.; Hanson, W. L. *Proc. Natl. Acad. Sci. U.S.A.* **1978**, *75*, 2959−2963.
(5) Leserman, L. D.; Barbet, J.; Kourilsky, F.; Weinstein, J. N. *Nature* **1980**, *288*, 602−604.
(6) Heath, T. D.; Fraley, R. T.; Papahadjopoulos, D. *Science* **1980**, *210*, 539−541.
(7) Gabizon, A.; Chisin, R.; Amselem, S.; Druckmann, S.; Cohen, R.; Goren, D.; Fromer, I.; Peretz, T.; Sulkes, A.; Barenholz, Y. *Br. J. Cancer* **1991**, *64*, 1125−1132.
(8) Monsky, W. L.; Fukumura, D.; Gohongi, T.; Ancukiewcz, M.; Weich, H. A.; Torchilin, V. P.; Yuan, F.; Jain, R. K. *Cancer Res.* **1999**, *59*, 4129−4135.
(9) Gabizon, A.; Goren, D.; Cohen, R.; Barenholz, Y. *J. Controlled Release* **1998**, *53*, 275−279.
(10) Litzinger, D. C.; Buiting, A. M.; van Rooijen, N.; Huang, L. *Biochim. Biophys. Acta* **1994**, *1190*, 99−107.

10.1021/ja056719u CCC: $33.50

(i) they readily form vesicles when the polymer is hydrated,[11−13] (ii) the average size of these vesicles can be controlled by extrusion,[13,14] (iii) they are easy to modify chemically,(iv) they can encapsulate molecules and incorporate large proteins into their membrane,[15−19] and (v) they have shown to be promising carriers in targeted drug delivery.[20]

Assaying successful targeted drug delivery by using fluorescent techniques has up to now been limited to analysis by fluorimetry, fluorescent activated cell sorting (FACS), and confocal laser scanning microscopy (CLSM) and other emerging fluorescent methods.[21−25] Clearly, alternative powerful analytical tools are needed to elucidate the precise molecular interactions taking place during cellular targeted drug delivery. By using fluorescence correlation spectroscopy (FCS) and fluorescence cross-correlation spectroscopy (FCCS) the number, the diffusion properties, and the molecular brightness of the molecular species can be determined.[26−28] A major advantage of FCS is its possibility to determine in situ parameters such as binding constants and reaction rates with high sensitivity compared to that of other fluorescent techniques such as CLSM and FACS.

In this study, an ABA triblock copolymer consisting of two hydrophilic blocks A (polymethyloxazoline, PMOXA) and a hydrophobic block B (poly(dimethylsiloxane), PDMS) and derivatives thereof were used to prepare nanometer-sized vesicles, so-called nanocontainers (NCs), with encapsulated low molecular weight fluorescent dyes or fluorescent proteins. When hydrated, the block copolymer forms vesicles with a specific size distribution. Different spectroscopic techniques such as CLSM and FCS were used to study these containers in more detail. FCS enables us to determine the size, the size distribution, and the number of encapsulated fluorescently labeled proteins. Comparison with photon correlation spectroscopy (PCS) was done in order to determine the accuracy and reproducibility of results obtained by FCS. Moreover, titration of biotinylated fluorescent NCs to fluorescently labeled streptavidin studied with FCCS enables the precise quantification of the interaction that takes place at the surface of the NCs. These results may pave the way to a better understanding of the molecular interactions underlying the transduction pathway in cellular targeted drug delivery.

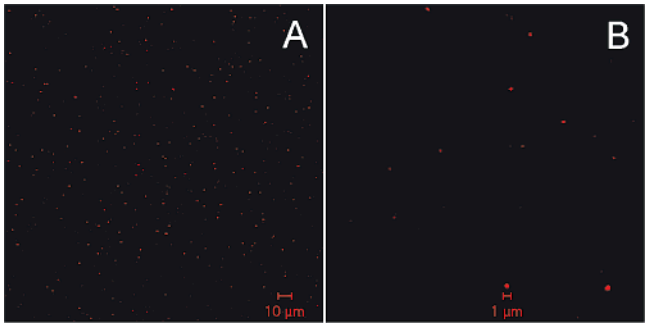

Figure 1. Fluorescence micrographs of NCs labeled with SRB. (A) Sample of polymeric NCs prepared with a starting concentration of 30 mM SRB by excitation with a 543 nm laser without zoom and (B) using 5.6 times optical zoom.

Results and Discussion

Imaging Polymeric Fluorescent NCs. Fluorescent polymeric NCs, using the triblock copolymer JW 05, were prepared using a previously published protocol (see the Supporting Information for details). In general, polymeric NCs independently of the preparation method have a size which is around or below the resolution limit of the confocal microscope[29] (approximately 250 nm) making acquisition of fluorescence micrographs a difficult task. Although the particles are below the resolution limit they can be detected under epi-illumination with the proper beam line as fluorescent dots diffusing through the focus indicating that the fluorophore is either encapsulated or otherwise associated to the NC. NCs without encapsulated fluorophore are not visible. On the other hand, NCs labeled with the dye sulforhodamine B (SRB) are readily detectable by a CLSM (Figure 1). Fluorescence micrographs were acquired from NCs labeled by using different starting concentrations of SRB. As determined from analysis of the micrographs the size of the particles is independent of the concentration of the fluorescent dye which is also corroborated by the results obtained from FCS analysis (see Table 1). Furthermore, image analysis shows that there is very little free dye in the sample which also corresponds well with data obtained by FCS. The apparent size of the fluorescent NCs, less than 1 μm in diameter, can be seen in Figure 1B. This value is in agreement with the values obtained by either FCS or PCS (see Table 1, Supporting Information). Since both FCS and PCS delivers average values of the hydrodynamic radius, larger particles occasionally detected by CLSM are probably due to aggregation of single NCs or other bigger colloidal aggregates.

Encapsulation of Small Dye Molecules by NCs. In drug delivery a major concern is to establish new methods to determine the encapsulation efficiency of the active drug. Here, encapsulation was determined by using FCS on polymeric NCs containing organic dye molecules or fluorescent proteins.

SRB is a readily water-soluble analogue of the rhodamine dye, with an excitation and emission maximum at 565 and 586 nm, respectively. A dilute aqueous solution of SRB (10 nM) was analyzed by FCS using the 543 nm laser line. High

(11) Zhang, L. F.; Eisenberg, A. *Science* **1995**, *268*, 1728−1731.
(12) Vanhest, J. C. M.; Delnoye, D. A. P.; Baars, M. W. P. L.; Vangenderen, M. H. P.; Meijer, E. W. *Science* **1995**, *268*, 1592−1595.
(13) Discher, D. E.; Eisenberg, A. *Science* **2002**, *297*, 967−973.
(14) Soo, P. L.; Eisenberg, A. *J. Polym. Sci., Part B: Polym. Phys.* **2004**, *42*, 923−938.
(15) Meier, W.; Nardin, C.; Winterhalter, M. *Angew. Chem., Int. Ed.* **2000**, *39*, 4599−4602.
(16) Sauer, M.; Haefele, T.; Graff, A.; Nardin, C.; Meier, W. *Chem. Commun.* **2001**, 2452−2453.
(17) Winterhalter, M.; Hilty, C.; Bezrukov, S. M.; Nardin, C.; Meier, W.; Fournier, D. *Talanta* **2001**, *55*, 965−971.
(18) Graff, A.; Sauer, M.; Van Gelder, P.; Meier, W. *Proc. Natl. Acad. Sci. U.S.A.* **2002**, *99*, 5064−5068.
(19) Stoenescu, R.; Graff, A.; Meier, W. *Macromol. Biosci.* **2004**, *4*, 930−935.
(20) Broz, P.; Benito, S. M.; Saw, C.; Burger, P.; Heider, H.; Pfisterer, M.; Marsch, S.; Meier, W.; Hunziker, P. *J. Controlled Release* **2005**, *102*, 475−488.
(21) Hege, K. M.; Daleke, D. L.; Waldmann, T. A.; Matthay, K. K. *Blood* **1989**, *74*, 2043−2052.
(22) Touitou, E.; Godin, B.; Dayan, N.; Weiss, C.; Piliponsky, A.; Levi-Schaffer, F. *Biomaterials* **2001**, *22*, 3053−3059.
(23) Nitin, N.; Santangelo, P. J.; Kim, G.; Nie, S.; Bao, G. *Nucleic Acids Res.* **2004**, *32*, e58.
(24) Sauer, I.; Dunay, I. R.; Weisgraber, K.; Bienert, M.; Dathe, M. *Biochemistry* **2005**, *44*, 2021−2029.
(25) Tanke, H. J.; Dirks, R. W.; Raap, T. *Curr. Opin. Biotechnol.* **2005**, *16*, 49−54.
(26) Rigler, R.; Mets, U.; Widengren, J.; Kask, P. *Eur. Biophys. J.* **1993**, *22*, 169−175.
(27) Schwille, P.; Meyer-Almes, F. J.; Rigler, R. *Biophys. J.* **1997**, *72*, 1878−1886.
(28) Rigler, R.; Foldes-Papp, Z.; Meyer-Almes, F.-J.; Sammet, C.; Volcker, M.; Schnetz, A. *J. Biotechnol.* **1998**, *63*, 97−109.
(29) Keller, H. E. In *Handbook of Confocal Microscopy*; Pawley, J. B., Ed.; Plenum Press: New York, 1995; pp 111−126.

Table 1. FCS Evaluation of NCs Labeled with SRB[a]

sample	CR [kHz]	CPM [kHz]	N[b]	F_1 [%], $\tau_{D,1}$ [μs][c]	F_2 [%], $\tau_{D,2}$ [ms][c]	F_3 [%], $\tau_{D,3}$ [ms][c]
NCs, 3 mM SRB[d]	198 ± 3	1466 ± 174	0.14 ± 0.05	1 ± 1, 30	28 ± 15, 2.27 ± 1.43	71 ± 13, 9.68 ± 1.67
NCs, 300 μM SRB[d]	15 ± 5	1030 ± 140	0.02 ± 0.01	1 ± 1, 30	20 ± 11, 2.02 ± 1.32	79 ± 11, 8.02 ± 1.78
SRB, 10 nM[e]	9	20	0.4	100, 30	NA[f]	NA[f]

[a] Experiments performed by excitation with a 543 nm HeNe laser. [b] N, number of molecules/particles in detection volume. [c] F_n, fraction of molecules/particles having a specific diffusion time. [d] SRB, starting concentration of sulforhodamine B. [e] SRB concentration of the free dye. [f] Not applicable.

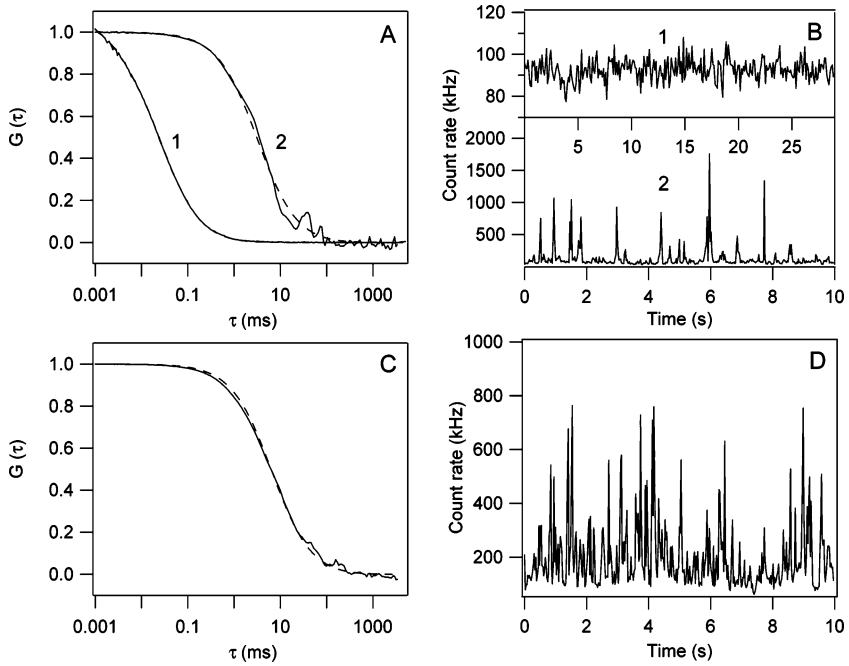

Figure 2. FCS data obtained by measuring polymeric NCs labeled with SRB. (A) Normalized autocorrelation curves and (B) fluorescence intensity traces of (1) free SRB and (2) SRB encapsuled in NCs, respectively. Note that the ordinate scales of the different curves in (B) are different. (C) Normalized autocorrelation curve and (D) fluorescence intensity trace of SRB encapsulated in NCs acquired by averaging 10 measurements of 10 s duration. The dashed curves in (A) and (C) are obtained by fitting the autocorrelation data. The initial SRB concentrations for free dye and NCs were 10 nM and 3 mM, respectively.

molecular brightness values, here expressed as counts per molecule (CPM), of around 100 kHz are readily achieved while simultaneously obtaining low triplet state population (10%) and an appropriate aspect ratio ($R = 6$) of the confocal detection volume. The diffusion time for SRB is 26 μs. Figure 2 shows data obtained by measuring polymeric NCs labeled with SRB using the 543 nm laser line. The graphs in the upper panel show the fluorescence intensity traces of freely diffusing SRB and SRB encapsulated in NCs. Comparison of the average count rate clearly indicates that NCs have a fluorescence intensity which is significantly higher than that of the free dye. The aforementioned NCs also give rise to significant intensity bursts (trace 2 Figure 2B) which vary in peak intensity and width reflecting different molecular brightness and size, respectively. Parts C and D of Figure 2 show that it is very important to acquire data long enough to obtain smoother autocorrelation curves. Differences in intensity bursts can also be accounted for by particles diffusing via different trajectories through the Gaussian excitation volume. The differences in intensity can also be due to particles containing more or less fluorescent dye. The detailed results of these measurements are listed in Table 1.

FCS results indicate that only a negligible part of the sample corresponds to free SRB (Table 1). It should however be noted that the fraction of freely diffusing dye could be significantly underestimated since its molecular brightness and thus its fluorescence quantum yield is considerably lower than that of the fluorescent NC.[30,31] Preliminary results (data not shown) obtained from fluorescent intensity distribution analysis (FIDA) on the intensity traces obtained with the FCS setup indicate that the fraction of free dye is significantly higher than the values obtained by fitting the autocorrelation curves. On the other hand, FIDA analysis results in molecular brightness of fluorescent NCs matching those acquired by autocorrelation curve fitting. NCs give rise to particles which have an intermediate diffusion time of 2.1 ms (25% in average), but the majority of particles (75%) have a diffusion time of 8.9 ms. Measurements performed more than 1 month later with NCs resulted in similar values indicating the excellent stability of these polymeric NCs.

The diffusion time obtained from FCS can also be used to determine the hydrodynamic radius, R_h, of the particles by using the Stokes−Einstein relation, $D = k_B T/6\pi\eta R_h$, where D is the diffusion coefficient which is related to k_B, the Boltzmann constant, T, the temperature, η, the viscosity, and R_h as described in the above equation. Earlier work comparing FCS, photon correlation spectroscopy (PCS), and TEM measurements on latex beads indicate that FCS delivers accurate determination of R_h.[32] An effect which might influence the determination of

(30) Rauer, B.; Neumann, E.; Widengren, J.; Rigler, R. *Biophys. Chem.* **1996**, *58*, 3−12.
(31) Meseth, U.; Wohland, T.; Rigler, R.; Vogel, H. *Biophys. J.* **1999**, *76*, 1619−1631.

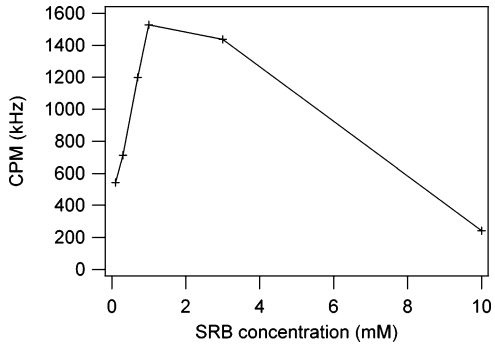

Figure 3. Sulforhodamine (SRB) encapsulation by polymeric NCs. Molecular brightness, here expressed as counts per molecule (CPM), of fluorescent NCs is plotted vs the starting concentration of SRB used for the preparation of the NCs. The line indicates the calculated best fit to the experimental data.

hydrodynamic radius by FCS is photobleaching.[33] Absence of any significant dependence on the observed diffusion times of the intensity of the laser light suggests that photobleaching is not significant in our studies. Our fluorescently labeled NCs lead to particles which have an R_h of 86 nm. Furthermore, this work shows that as the particle size gets bigger (radius of particle $> 0.2\omega_{xy}$[34]) the apparent R_h as determined by FCS starts to deviate from that obtained by PCS and theoretical considerations. We verified the accuracy of the hydrodynamic radii determined by FCS, by measuring fluorescent polystyrene beads with radii of 20, 50, and 100 nm (Table 1, Supporting Information). The agreement is good for the smaller particles ($R_{h,FCS,20nm} = 20 \pm 4$ nm and $R_{h,FCS,50nm} = 54 \pm 11$ nm) but is worse for the 100 nm particles ($R_{h,FCS,100nm} = 354 \pm 134$ nm) which is mainly dependent on aggregation of latex beads since PCS measurements of the same particles resulted in similarly large numbers (see below). PCS analysis was also performed to determine the hydrodynamic radius of the polystyrene beads. The obtained values for the 20 and 50 nm polystyrene beads are 26 and 60 nm, respectively, and compare well with those obtained by FCS.[35−37] The 100 nm polystyrene beads resulted in hydrodynamic radii of almost 400 nm indicating aggregation of particles.

SRB at different starting concentrations (300 μM and 1, 3, and 10 mM) was encapsulated in polymeric NCs in order to obtain a calibration curve enabling the determination of the amount of fluorescent dye per NC. In Figure 3 the determined molecular brightness, here given as CPM, is plotted as a function of the starting concentration of the dye solution of SRB. The molecular brightness increases from 542 kHz (100 μM SRB) to 1528 kHz (1 mM SRB), then levels off, and finally drops down to 242 kHz (10 mM SRB) (Figure 3). Two important results emanate from these measurements: (i) the relationship between molecular brightness and the starting concentration of the dye is linear in the beginning, and (ii) the initial slope of the line indicates that dye loading is lower than expected. Furthermore, the molecular brightness levels off at 1 mM SRB and corresponds well with the non-self-quenching value used by others.[38] Clearly, the optimal dye loading range starts at a concentration corresponding to the sensitivity limit of detecting fluorescently labeled NCs with high enough signal-to-noise ratio (50 μM) and ends with a concentration most probably associated with self-quenching of dye molecules (1 mM). How does the molecular brightness compare to the actual number of dye molecules per NC particle? Preparation of NCs with 1 mM SRB would correspond to more than 3×10^3 dye molecules in an NC with a diameter of about 150 nm. Since the molecular brightness of the freely diffusing dye is known it can be used to determine the number of encapsulated dye molecules if the assumption is made that there is no significant photobleaching and the detector is not saturated. The measured molecular brightness of the freely diffusing SRB and that of NCs prepared with 1 mM SRB is about 100 kHz and 1528 kHz, respectively, indicating that NCs contain only about 15 dye molecules. The large discrepancy between the expected and the experimentally determined number of encapsulated dye molecules is most probably due to self-quenching between the tightly packed dye molecules inside the NCs.[39] Another plausible explanation would be that dye molecules are excluded from the interior of the NC. This explanation is most probably not applicable since the measurements with encapsulation of avidin−Alexa 488 show that encapsulation efficiency is good.

Encapsulation of Fluorescent Proteins by NCs. A lot of research has been carried out on the encapsulation of proteins by phospholipid vesicles in comparison to methods using similarly sized polymeric containers.[40−42] To show the versatility of our polymeric NCs for encapsulation of molecules we also encapsulated fluorescent proteins such as avidin labeled with the fluorophore Alexa 488. NCs were prepared with a starting concentration of 1 mg/mL avidin−Alexa 488. Figure 4 depicts the results obtained from measuring NCs labeled with avidin−Alexa 488. The upper graph shows the fluorescence intensity trace containing several bursts reaching intensity values over 250 kHz with most having values ranging from 100 to 150 kHz corresponding to single NCs diffusing through the detection volume. Bleaching effects can be neglected since the NCs diffuse quickly enough through the detection volume, and saturation effects of the detector can also be disregarded since the measured intensity values are significantly below the saturation level of the avalanche photodiode detector.

Figure 4B shows the autocorrelation curves of freely diffusing Alexa 488, avidin−Alexa 488, and NCs with encapsulated avidin−Alexa 488. Alexa 488 is a highly photostable fluorophore which has a quite high molecular brightness (counts per molecule (CPM) = 53 kHz), is readily water-soluble, and has a characteristic diffusion time of 27 μs. Upon conjugation of Alexa 488 to the 66 kDa protein avidin, the characteristic diffusion time increases to 142 μs and the molecular brightness drops to 36 kHz which is mostly attributed to quenching of the

(32) Starchev, K.; Zhang, J. W.; Buffle, J. *J. Colloid Interface Sci.* **1998**, *203*, 189−196.
(33) Lead, J. R.; Balnois, E.; Hosse, M.; Menghetti, R.; Wilkinson, K. J. *Environ. Int.* **1999**, *25*, 245−258.
(34) ω_{xy} is the radial dimension of the fluorescence excitation volume.
(35) Starchev, K.; Buffle, J.; Perez, E. *J. Colloid Interface Sci.* **1999**, *213*, 479−487.
(36) Bonné, T. B.; Lüdtke, K.; Jordan, R.; Stepanek, P.; Papadakis, C. M. *Colloid Polym. Sci.* **2004**, *282*, 833−843.
(37) Xu, H.; Frank, J.; Trier, U.; Hammer, S.; Schroder, W.; Behlke, J.; Schafer-Korting, M.; Holzwarth, J. F.; Saenger, W. *Biochemistry* **2001**, *40*, 7211−7218.
(38) Sonawane, N. D.; Thiagarajah, J. R.; Verkman, A. S. *J. Biol. Chem.* **2002**, *277*, 5506−5513.
(39) Tsien, R. Y.; Waggoner, A. In *Handbook of Biological Confocal Microscopy*; Pawley, J. B., Ed.; Plenum Press: New York, 1995; pp 267−280.
(40) Phillips, N. C.; Emili, A. *Vaccine* **1992**, *10*, 151−158.
(41) Fries, L. F.; Gordon, D. M.; Richards, R. L.; Egan, J. E.; Hollingdale, M. R.; Gross, M.; Silverman, C.; Alving, C. R. *Proc. Natl. Acad. Sci. U.S.A.* **1992**, *89*, 358−362.
(42) Walde, P.; Ichikawa, S. *Biomol. Eng.* **2001**, *18*, 143−177.

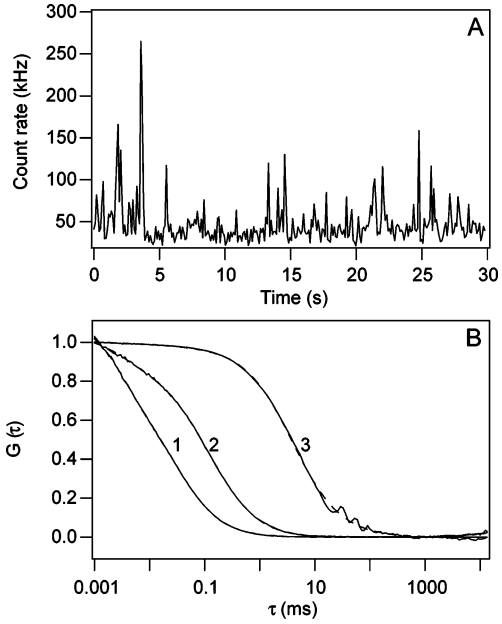

Figure 4. FCS data of NCs labeled with avidin−Alexa 488. (A) Fluorescence intensity trace of NCs and (B) autocorrelation curves of (1) free Alexa 488, (2) avidin−Alexa 488, and (3) NCs labeled with avidin−Alexa 488 and their corresponding fitted curves (dashed lines).

dye.[43] The determined diffusion time of avidin−Alexa 488, 142 μs, corresponds to a hydrodynamic radius of 2.6 nm which is in excellent agreement with the calculated radius, 2.8 nm, by using a molecular mass of 67 kDa for avidin−Alexa 488. The labeled NCs have a diffusion time of 3.8 ms, corresponding to a hydrodynamic radius of about 70 nm, and a molecular brightness of 350 kHz indicating that about 10 avidin−Alexa 488 molecules are encapsulated inside the polymeric NC. This value is in excellent agreement with the 13 avidin molecules, which represents the maximal theoretical number of encapsulated proteins by a sphere of 70 nm radius considering an avidin concentration of 1 mg/mL and a molecular weight of 67 000 g/mol. Additionally, experiments were performed where the starting concentration of avidin−Alexa 488 was varied from 0.03 to 1.0 mg/mL in order to determine the encapsulation efficiency with increasing concentration of avidin−Alexa 488. The number of avidin−Alexa 488 per NC for each sample was determined by taking the molecular brightness of the NC (here expressed as CPM) and dividing it with that of freely diffusing avidin−Alexa 488 ($CPM_{avidin-Alexa488}$ = 36 kHz). Figure 5 depicts the linear relationship between the number of encapsulated avidin−Alexa 488 and the starting concentration of the same protein. These findings indicate that the encapsulation efficiency of proteins is very high when preparing NCs with our triblock copolymer.

Binding of Labeled Avidin/Streptavidin to Biotinylated NCs. Biotin and avidin or streptavidin form one of the strongest noncovalent interactions with a dissociation constant between 10^{-15} and 10^{-13} M.[44,45] This ligand−receptor pair has proven to be enormously versatile in applications involving protein recognition of biotinylated molecules such as lipids, nucleic

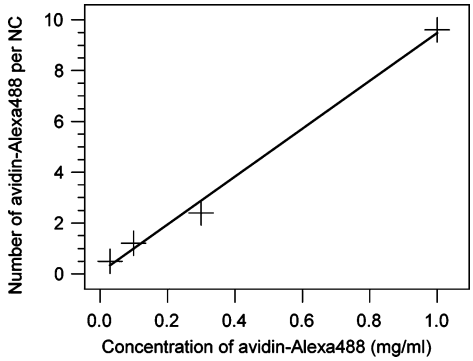

Figure 5. Determination of the number of avidin−Alexa 488 molecules per nanocontainer. The number of avidin−Alexa 488, which was obtained by dividing the molecular brightness of each sample with that of freely diffusing avidin−Alexa 488, is plotted against the starting concentration of avidin−Alexa 488. The line indicates the best calculated fit to the experimental data.

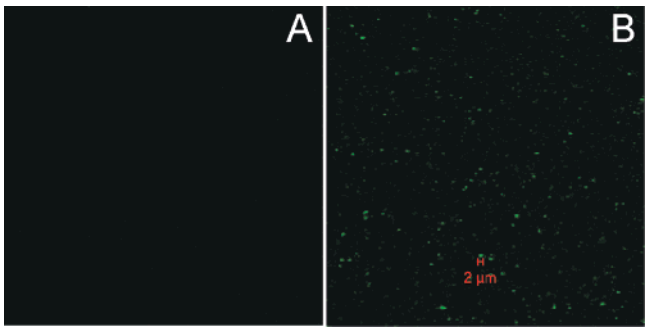

Figure 6. Specific binding of fluorescently labeled avidin (avidin−Alexa 488) to biotinylated polymeric nanocontainers. Fluorescence micrographs obtained by a confocal laser scanning microscope of biotinylated nanocontainers before addition of avidin−Alexa 488 (A) and after incubation with avidin−Alexa 488 (B).

acids, proteins, polymers, and nanoparticles.[46−52] Furthermore, biotinylated nano- and microparticles have been used as a model system to study protein−cell and cell−cell interactions, indicating the ubiquitous importance of performing such measurements in basic and applied research.[20,53,54]

Polymeric NCs were also prepared by mixing the parent triblock copolymer with its biotinylated analogue in a 10/1 ratio thereby producing biotinylated polymeric NCs. To determine the number of available biotin groups on the NC and to study the binding of the biotinylated NC with other molecules experiments were performed by adding fluorescent avidin (avidin−Alexa 488). Figure 6A shows confocal micrographs of biotinylated NCs before, and Figure 6B after, binding of excess avidin−Alexa 488. Images acquired from samples where avidin−Alexa 488 was added to NCs previously incubated with

(43) Rajagopalan, P. T.; Zhang, Z.; McCourt, L.; Dwyer, M.; Benkovic, S. J.; Hammes, G. G. *Proc. Natl. Acad. Sci. U.S.A.* **2002**, *99*, 13481−13486.
(44) Takeuchi, T.; Tham, S. Y.; Rechnitz, G. A. *Anal. Chim. Acta* **1991**, *251*, 291−295.
(45) Kuntz, I. D.; Chen, K.; Sharp, K. A.; Kollman, P. A. *Proc. Natl. Acad. Sci. U.S.A.* **1999**, *96*, 9997−10002.
(46) Helm, C. A.; Knoll, W.; Israelachvili, J. N. *Proc. Natl. Acad. Sci. U.S.A.* **1991**, *88*, 8169−8173.
(47) Vaknin, D.; Alsnielsen, J.; Piepenstock, M.; Losche, M. *Biophys. J.* **1991**, *60*, 1545−1552.
(48) Yin, H.; Landick, R.; Gelles, J. *Biophys. J.* **1994**, *67*, 2468−2478.
(49) Cannizzaro, S. M.; Padera, R. F.; Langer, R.; Rogers, R. A.; Black, F. E.; Davies, M. C.; Tendler, S. J. B.; Shakesheff, K. M. *Biotechnol. Bioeng.* **1998**, *58*, 529−535.
(50) Gref, R.; Couvreur, P.; Barratt, G.; Mysiakine, E. *Biomaterials* **2003**, *24*, 4529−4537.
(51) Lin, J. J.; Silas, J. A.; Bermudez, H.; Milam, V. T.; Bates, F. S.; Hammer, D. A. *Langmuir* **2004**, *20*, 5493−5500.
(52) Qi, K.; Ma, Q.; Remsen, E. E.; Clark, C. G., Jr.; Wooley, K. L. *J. Am. Chem. Soc.* **2004**, *126*, 6599−6607.
(53) Lee, H.; Kim, T. H.; Park, T. G. *J. Controlled Release* **2002**, *83*, 109−119.
(54) Nobs, L.; Buchegger, F.; Gurny, R.; Allemann, E. *Eur. J. Pharm. Biopharm.* **2004**, *58*, 483−490.

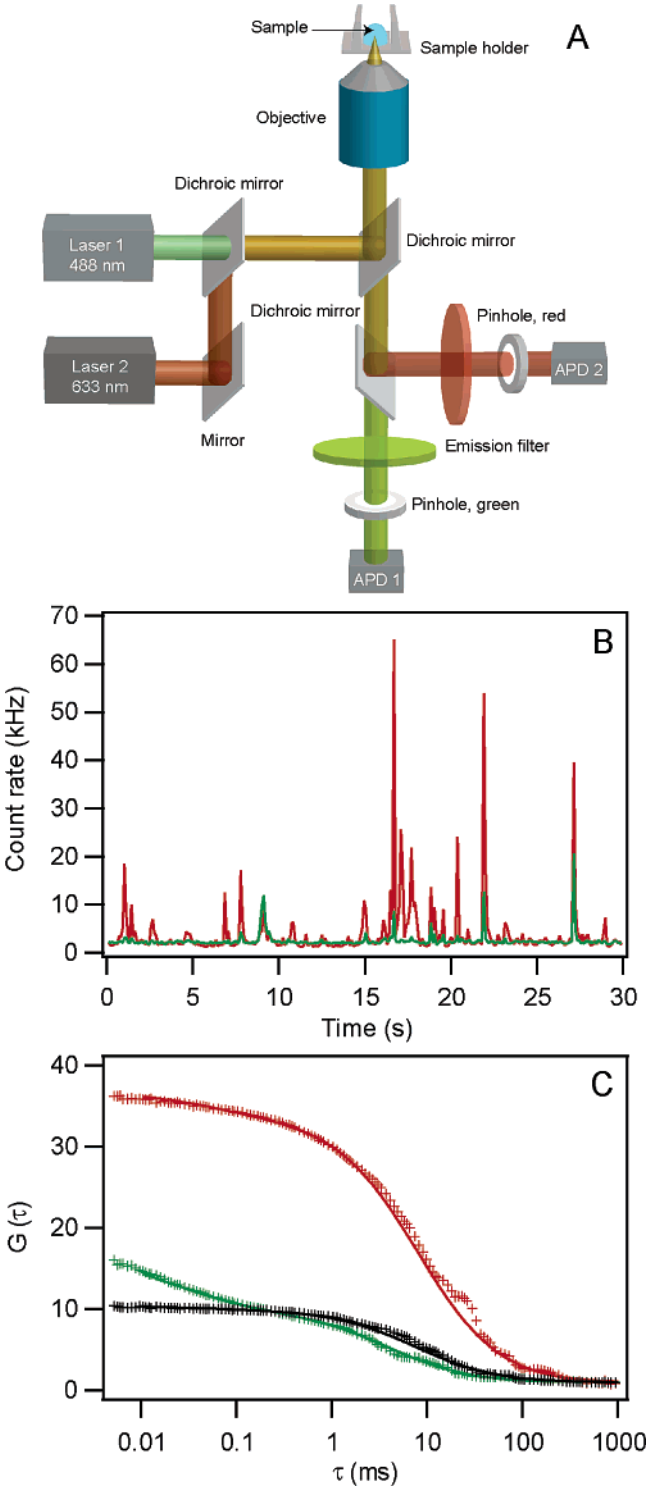

Figure 7. Beam path of the cross-correlation setup and experimental data obtained from SA−Cy5 bound to RhG-labeled NCs (double-labeled NCs). (A) Schematic diagram of the beam path of the dual-laser cross-correlation setup. (B) Graph showing experimental cross-correlation data in the form of count rates for the double-labeled NCs measured in the green detector (green line) and red detector (red line). (C) Red and green markers showing the autocorrelation curves measured in the red and green detector, respectively, and black markers showing the corresponding cross-correlation curve. Fitted curves are shown as solid lines.

an excess of biotin, to block all binding sites, correspond to the image in Figure 6A. Furthermore, control experiments with NCs without biotinylated polymers did not result in the typical

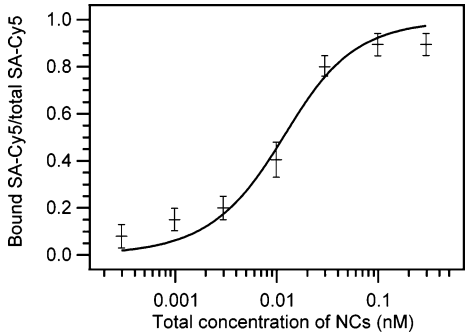

Figure 8. Determination of the number of streptavidin per NC and the dissociation constant of streptavidin−cyanin5 (SA−Cy5) to rhodamine-green-labeled biotinylated polymeric NCs (NC−RhG). Data points were obtained by plotting the fraction of bound SA−Cy5 vs the total concentration of NC−RhG. The solid line represents the fit to the experimental data by using eq 10 (see the Supporting Information), and error bars correspond to the standard deviation of two independent experiments.

fluorescent NCs seen in Figure 6A. These results clearly indicate that the interaction is specific to the biotin−avidin interaction.

In a recent publication, FCS was used to study receptor interactions for a system consisting of biotinylated shell cross-linked nanoparticles and avidin labeled with Oregon green 488, indicating that it is possible to determine the increase in the amount of available binding sites by following the increase in diffusion time as a function of biotin-terminated block copolymer concentration.[52]

Here, a model system comprising rhodamine-green-labeled biotinylated NCs (NC−RhGs) and cyanin5-labeled streptavidin (SA−Cy5) was utilized in order to determine the number of binding sites and the dissociation constant, K_d, of the receptor interaction between NC−RhG and SA−Cy5. To determine the number of available biotin groups on the surface of the NCs and the K_d of the system, a commercially available fluorescence cross-correlation spectroscopy (FCCS) setup was used to study the titration of NC−RhGs to a constant concentration of SA−Cy5 (Figure 7A). FCCS enables the independent determination of both single- and double-labeled species, i.e., the correlation amplitudes of SA−Cy5, NC−RhG, and SA−Cy5 bound to NC−RhGs can simultaneously be assessed (Figure 7B). The corresponding concentrations are obtained from the correlation amplitudes and the detection volume (see the Supporting Information for details). To evaluate the number of binding sites per NC and the intrinsic dissociation constant of the NCs for SA−Cy5, the fraction of bound SA−Cy5 was plotted against the total concentration of NC−RhG, and the experimental data were fitted with eq 10 (Figure 8). The number of binding sites per NC was determined to 1921 ± 357, whereas K_d yielded a value of $1.7 \pm 0.4 \times 10^{-8}$ M with the latter value corresponding well with data obtained from streptavidin-coated polystyrene beads.[55] The estimated number of binding sites, 1260, which was obtained by assuming an NC with a diameter of 200 nm, a surface area per polymer of 10 nm,[2,56] and the knowledge that only 10% of the total polymer is biotinylated, corresponds rather well with the value determined by FCCS considering the number of data points used for the fit. The intrinsic dissociation constant, K_d, of $1.7 \pm 0.4 \times 10^{-8}$ of each binding site should

(55) Buranda, T.; Jones, G. M.; Nolan, J. P.; Keij, J.; Lopez, G. P.; Sklar, L. A. *J. Phys. Chem. B* **1999**, *103*, 3399−3410.
(56) Nardin, C.; Hirt, T.; Leukel, J.; Meier, W. *Langmuir* **2000**, *16*, 1035−1041.

be compared to the literature value which ranges between 10^{-15} and 10^{-13} M. This discrepancy is most probably related to (i) an entropic effect arising from the immobilization of the biotin group at the surface of the NC and (ii) to a steric effect associated with a possible hindrance of the biotin binding site by surrounding polymer brushes but also to an inhibition of the ability of biotin to settle in the most stable position inside the binding pocket.

Conclusion

We have shown that it is possible to use FCS and FCCS to measure fluorescent polymeric NCs. The very high sensitivity of FCS enables high signal-to-noise ratio measurements of very low concentrations of fluorescently labeled NCs thereby reducing significantly the starting concentration of the often precious dye. Furthermore, we have shown that with FCS it is possible to determine the relative amount of encapsulated dye molecules and that high encapsulation efficacy can be achieved by using the appropriate preparation protocol. FCS can also be used to determine the size of the particles: fluorescently labeled polymeric NCs have a hydrodynamic radius ranging between 70 and 86 nm. Accurate determination of dye loading was demonstrated by encapsulating avidin−Alexa 488 in polymeric NCs. At 1 g/L avidin−Alexa 488 starting concentration about 10 labeled protein molecules can be detected inside the NC corresponding to an efficient encapsulation. Finally, we have shown that it is possible to determine the molecular interaction between biotinylated RhG-labeled NCs and fluorescently labeled protein, SA−Cy5, by using FCCS. The intrinsic dissociation constant of SA−Cy5 to the biotinylated NCs is $1.7 \pm 0.4 \times 10^{-8}$ M, and every NC is in average covered with 1921 ± 357 SA−Cy5 molecules. These results indicate that it is possible to use FCS and FCCS to study complex molecular interaction between 160 nm large fluorescently labeled polymeric NCs and proteins, paving the way for measurements enabling a quantitative elucidation of complex drug delivery mechanisms.

Acknowledgment. Per Rigler thanks Samantha Benito for helpful advice concerning the use of amphiphilic block copolymers and the preparation of NCs, as well as Professor Rudolf Rigler for many interesting and useful discussions concerning fluorescence fluctuation spectroscopy. Financial support from the company ZEISS, the Swiss National Science Foundation, the National Center for Competence in Nanoscale Science, and BBW (No. 03.0244; EU MRTN-CT-2003-505027) is also gratefully acknowledged.

Supporting Information Available: Experimental details and table showing size determination of fluorescent nanocontainers. This material is available free of charge via the Internet at http://pubs.acs.org.

JA056719U